



UNIVERSITY OF LEEDS

This is a repository copy of *Identifying the effects of land use change on sediment export: Integrating sediment source and sediment delivery in the Qiantang River Basin, China*.

White Rose Research Online URL for this paper:
<http://eprints.whiterose.ac.uk/146518/>

Version: Accepted Version

Article:

Zhou, M, Deng, J, Lin, Y et al. (5 more authors) (2019) Identifying the effects of land use change on sediment export: Integrating sediment source and sediment delivery in the Qiantang River Basin, China. *Science of the Total Environment*, 686. pp. 38-49. ISSN 0048-9697

<https://doi.org/10.1016/j.scitotenv.2019.05.336>

© 2019 Elsevier B.V. All rights reserved. This manuscript version is made available under the CC-BY-NC-ND 4.0 license <http://creativecommons.org/licenses/by-nc-nd/4.0/>.

Reuse

This article is distributed under the terms of the Creative Commons Attribution-NonCommercial-NoDerivs (CC BY-NC-ND) licence. This licence only allows you to download this work and share it with others as long as you credit the authors, but you can't change the article in any way or use it commercially. More information and the full terms of the licence here: <https://creativecommons.org/licenses/>

Takedown

If you consider content in White Rose Research Online to be in breach of UK law, please notify us by emailing eprints@whiterose.ac.uk including the URL of the record and the reason for the withdrawal request.



eprints@whiterose.ac.uk
<https://eprints.whiterose.ac.uk/>

Identifying the effects of land use change on sediment export: integrating sediment source and sediment delivery in the Qiantang River Basin, China

Deng J, Zhou M, Lin Y, Belete, M, Wang K, Comber A, Huang L and Gan M

Abstract

Dramatic land use change caused by the rapid economic development in China has impacted the sediment export dynamics in the large basin. However, how land use change affects sediment export is still poorly understood. This study provided an integrated analysis of the relationships in a “three-level” chain linked as follows: “land use change → changes in sediment source and sediment delivery → sediment export change” for a better understanding. It used the InVEST sediment delivery ratio (SDR) model to analyze the Qiantang River Basin ($4.27 \times 10^4 \text{ km}^2$), China. Sediment export change was examined from the two perspectives: the effects of land use change on sediment source and on sediment delivery. Correlations between changes in individual land use types and changes in sediment source and sediment delivery were identified. The results indicated that sediment export reduced from $1.69 \text{ t ha}^{-1} \text{ yr}^{-1}$ in 1990 to $1.22 \text{ t ha}^{-1} \text{ yr}^{-1}$ in 2015 because of the decreased sediment source and a weakened sediment delivery function. In the study area, the conversions of cropland to urban land (urbanization) and bare land to forestland (afforestation) were found to make the major contributions to reductions in soil loss and SDR, respectively. Furthermore, soil loss change resulted in the decreases in total value of sediment export and SDR change caused a large-scale spatial change in sediment export. Our hotspot analysis revealed that the Wuxi River watershed should be targeted for priority conservation to optimize land use/cover for reducing sediment export. This study demonstrates the benefits of taking a comprehensive approach to analyze the processes associated with sediment export change. These allow to improve sediment management and promote aquatic ecosystem health by providing specific future land use recommendations, aimed at source treatment and delivery interception.

Keywords: Land use change; Soil loss; Sediment delivery ratio; Sediment export; InVEST model

1 Introduction

China has experienced drastic land use change caused by rapid urbanization and land use policies since the market-directed economic system was implemented in 1992 (Liu et al., 2014; Liu et al., 2018). This has had significant influences on sediment export to rivers because of the change in surface roughness, soil infiltration rate and hydraulic connectivity within watersheds (Fiener et al., 2011; Tang et al., 2011). Redundant sediment export reduces soil fertility, water and nutrient retention capacity, and increases suspended solids in water. These threaten ecosystem health and increase the risk of reservoir sedimentation, reducing reservoir performance and increasing costs (Vanacker et al., 2003; Keeler et al., 2012).

39 Sediment export describes the amount of onsite sediment source actually reaching the
40 catchment outlet. It is determined by soil erosion from the land surface by rainfall–runoff as
41 well as sediment delivery processes based on land connectivity (Bakker et al. 2008; Vigiak et
42 al., 2012). It is also a function of land use as sediment transport capacities vary for different
43 land use types (Van Rompaey et al., 2001). Therefore, the impact of land use change on
44 sediment export can be divided into two parts: impacts on sediment source and on sediment
45 delivery. Recent watershed studies indicated that sediment export is affected by land use
46 change, soil and water conservation measures, and other anthropogenic activities (Walling
47 and Fang, 2003; Kondolf et al., 2014; Wang et al., 2016). Most of these studies have
48 emphasized the impacts of land use on soil erosion (sediment source) and sediment yield and
49 have sought to quantify the impacts reducing soil erosion as a control on the sediment yield
50 (Bakker et al., 2008; Fang, 2017; Romano et al., 2018). However, the impacts and
51 contribution of land use changes on sediment delivery and export are still poorly understood.
52 Few studies have considered the integrated “three-level” chain of “land use change →
53 changes in sediment source and sediment delivery → sediment export change”, that is the
54 relationships between changes in land use, sediment export and sediment source and delivery
55 (Alatorre et al., 2012; Shi et al., 2012). Research in these areas is necessary to fill gaps in
56 knowledge and understanding of sediment export processes and thereby to better support
57 sediment control.

58 Sediment source and sediment delivery (part 2 of the chain above) can be described as
59 soil loss and sediment delivery ratio (SDR) for the quantitative analysis. The revised
60 universal soil loss equation (RUSLE) by Renard et al. (1997) predicts soil loss owing to
61 water erosion as the main sediment source (Yang et al., 2003; Lu et al., 2004; Sun et al.,
62 2014). A number of studies have used RUSLE to examine soil loss driven by land use change
63 varying C and P factors with the land use changes but keeping other factors constant (e.g. soil
64 properties, topography and climatic features) (Erskine et al., 2002; Wei et al.; 2007). Some
65 researchers found that soil loss was more sensitive to changes in some key land use types
66 (such as forestland and cropland) than in other land use types (Feng et al., 2010; Rao et al.,
67 2016), suggesting the need to investigate the varying contributions to soil loss of different
68 land use changes. The SDR is the fraction of gross soil erosion that is transported to rivers
69 from a given catchment in a given time interval (Lu et al., 2006). Although many studies have
70 investigated on SDR considering its definition, contributing factors, calculation methods and
71 measurements (Vigiak et al., 2012; Woznicki and Nejadhashemi, 2013; Wu et al., 2013),
72 little work has examined the spatial variation in SDR and how it relates to land use change,
73 and how changes in individual land use types contribute to change in SDR at the watershed
74 scale.

75 In order to address these gaps, the InVEST (Integrated Valuation of Environmental
76 Services and Tradeoffs) sediment delivery ratio (SDR) model was applied in this study. This
77 model has been widely utilized in reservoir management and instream water quality
78 maintenance to map the overland sediment generation and delivery to streams (Hamel et al.,
79 2015; Hamel et al., 2017). This model has been shown to perform well after calibration with
80 the observation data, and has been successfully used to estimate sediment retention services

81 and describe the spatial distribution of sediment export (Sánchez-Canales et al., 2015; Jiang
82 et al., 2016). The resulting outputs include maps of soil loss, SDR and sediment export which
83 were used to analyze the relationships between land use and individual results. Such analysis
84 support understanding of how different land use changes contribute to sediment source and
85 sediment delivery, and therefore sediment export.

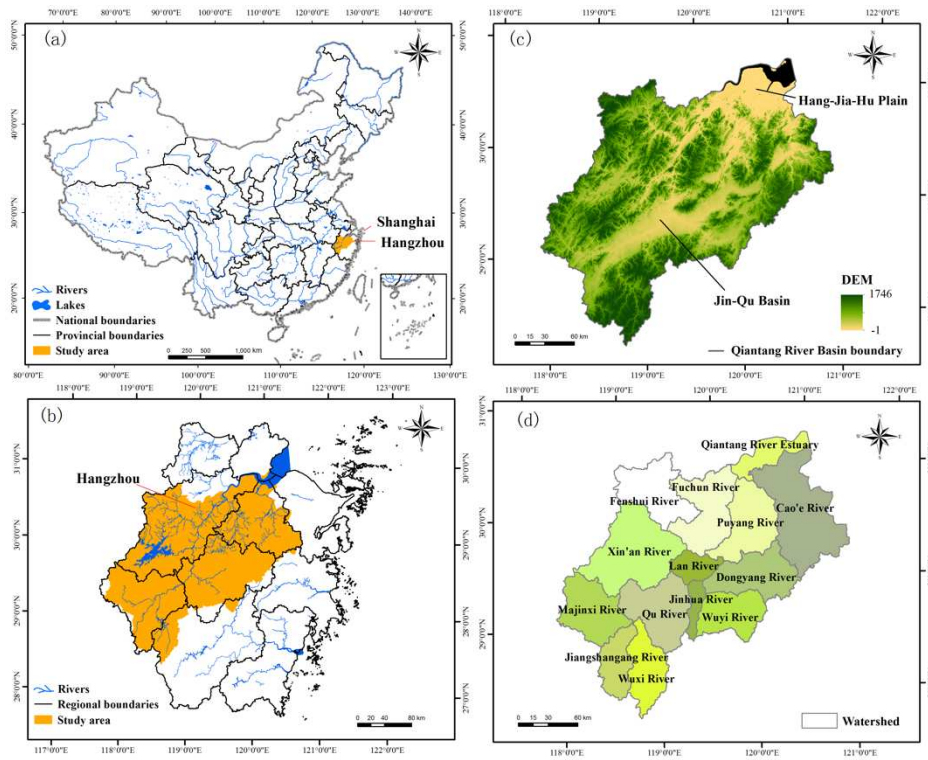
86 The Qiantang River Basin, located in southeast China, provides the strong soil
87 conservation services because of current land use/cover and erosion controls. However, it is
88 subject to high soil erosion risks due to the frequency of heavy rainfall and its mountainous
89 terrain which require greater consideration in future land use planning (Rao et al, 2014).
90 Since the 1990s, land use in the study basin has undergone dramatic changes because of
91 urbanization and specific land use policies. In our study, we attempt to explain sediment
92 export change caused by land use changes through analysis of changes in soil loss and SDR
93 using the InVEST SDR model. The objectives of this study are as follows: (1) to trace the
94 dynamics of soil loss, SDR and sediment export under different land use patterns from 1990
95 to 2015; (2) to analyze the relationships between soil loss, SDR and land use composition at
96 the sub-watershed level ($n = 763$); (3) to evaluate the impacts of changes in individual land
97 use types on soil loss and SDR and to identify the dominant contributors to changes in rates
98 of soil loss and SDR; (4) to explain the effects of changes in soil loss and SDR on sediment
99 export; (5) to propose practical recommendations for land use planning in support of
100 improved watershed management.

101 **2 Methods**

102 **2.1 Study area**

103 The Qiantang River Basin was in Zhejiang Province. Zhejiang Province is located in the
104 south of the Yangtze River Delta on the southeast coast of China and has a typical landscape
105 composition of ~70% mountains, ~10% water and ~20% fields (Fig. 1). It is one of the most
106 developed provinces in China and the Qiantang River is the largest river in the Province. The
107 basin has an area of 4.27×10^4 km² and is dominated by a typical subtropical humid monsoon
108 climate. The annual average air temperature is about 17°C and the annual precipitation is
109 about 1500 mm. In recent years, land use in the river basin has dramatically changed
110 especially urban land, cropland and forestland because of intensive human activities and land
111 protection policies (Fig. 2(a)). To explore the relationship between land use and sediment
112 export, the basin was divided into 14 watersheds and 763 sub-watersheds using Hydrology
113 tools in ArcGIS software based on a digital elevation model.

114



115

116 **Fig. 1.** Location of the study basin and watersheds: the location of the study basin in (a) China and (b)
 117 Zhejiang Province; (c) the elevation map of the study basin; (d) the distribution of the 14 watersheds.

118 2.2 Model description

119 Considering input data, complexity and model uncertainty, the InVEST SDR model was
 120 chosen. It calculates the sediment export by integrating a soil loss algorithm (Renard et al.,
 121 1997) with the sediment connectivity algorithm (Borselli et al., 2008), and generates maps of
 122 soil loss, SDR and sediment export as outputs. The main data requirements and sources in the
 123 model were represented in Table S1.

124 The sediment export ($t\ ha^{-1}\ yr^{-1}$) from a pixel i is given by:

$$125 \quad Sed_export_i = SL_i * SDR_i \quad (1)$$

126 Where SL_i is the average amount of annual soil loss ($t\ ha^{-1}\ yr^{-1}$) on a pixel i ; SDR_i is
 127 sediment delivery ratio for a pixel i . Ultimately, the total sediment yield in the catchment is
 128 the sum of sediment export from all pixels, which can be used to calibrate and validate the
 129 model.

130 Soil loss (SL) is computed with the RUSLE model (Renard et al., 1997):

$$131 \quad SL = R * K * LS * C * P \quad (2)$$

132 Where R is the rainfall erosivity ($MJ\ mm\ ha^{-1}\ h^{-1}\ yr^{-1}$); K is the soil erodibility ($t\ ha\ h\ ha^{-1}$
 133 $MJ^{-1}\ mm^{-1}$); LS is the slope length–gradient factor; C is the vegetation cover-management
 134 factor and P is the support practice factor.

135 SDR was calculated using the approach described in Vigiak et al. (2012), as a function of
 136 the hydrologic connectivity of the area derived from DEM. An index of connectivity, IC ,
 137 describes the degree of hydrological connectivity of a pixel to stream. Here it was measured
 138 by its upslope contribution and flow path to the stream (Borselli et al., 2008). The SDR can
 139 be computed as:

$$140 \quad SDR = \frac{SDR_{max}}{1 + \exp\left(\frac{IC_0 - IC}{k_b}\right)} \quad (3)$$

$$141 \quad IC = \log_{10} \left(\frac{D_{up}}{D_{dn}} \right) \quad (4)$$

$$142 \quad D_{up} = \bar{C}\bar{S}\sqrt{A} \quad (5)$$

$$143 \quad D_{dn} = \sum_i \frac{d_i}{C_i S_i} \quad (6)$$

144 Where SDR_{max} is the maximum theoretical SDR, adopting a default value of 0.8 (Vigiak et al.,
 145 2012); IC_0 and k_b are calibration parameters; D_{up} is the upslope component; D_{dn} is the
 146 downslope component; \bar{C} is the average C factor of the upslope contributing area; \bar{S} is the
 147 average slope gradient of the upslope contributing area ($m\ m^{-1}$); A is the upslope contributing
 148 area (m^2); d_i is the average length of the flow path along the i th cell according to the steepest
 149 downslope direction (m); C_i and S_i are the C factor and the slope gradient of the i th pixel,
 150 respectively. The upslope contributing area and the downslope flow path is delineated from
 151 the D-infinity flow routing algorithm (Tarboton, 1997).

152 **2.3 Parameters**

153 **2.3.1 Parameters in the RUSLE model**

154 The calculation methods of parameters in RUSLE model were received from the related
 155 researches (Sheng et al., 2010; Rao et al., 2014; Kong et al., 2018) and were detailed in Text
 156 S1. First, rainfall erosivity (R), as the primary factor in the RUSLE model, describes the
 157 potential of rainstorms to cause soil erosion (Wischmeier and Smith, 1978; Zhang et al.,
 158 2002). The annual rainfall erosivity, a raster generated by the Kriging interpolation of data

159 from 23 weather stations from 1990 to 2015, was calculated from the daily rainfall data using
160 half-month rainfall erosivity model proposed by Zhang et al. (2002) (Text S1). This model
161 was estimated using daily rainfall data and has been widely used in China (Xin et al., 2011;
162 Sun et al., 2014; Yang and Lu, 2015).

163 Next, the soil erodibility factor (K) reflects the sensitivity of soils to water erosion due to
164 soil properties (Zhang et al., 2008; Rao et al., 2014). In this paper, the soil erodibility factor
165 value was derived from the revised erosion/productivity impact calculator (EPIC) model
166 (Williams et al., 1984; Zhang et al., 2008) (Text S1).

167 The topographic factor (LS) captures the effect of slope length and slope gradient on soil
168 erosion (Wischmeier and Smith, 1978) and can be computed from a DEM (McCool et al,
169 1997; Renard et al., 1997) (Text S1).

170 The vegetation cover factor (C) is sensitive to natural and anthropogenic activities and is
171 critical to soil and water conservation (Wang et al., 2001). The value of C directly affects the
172 value of soil loss and SDR. Based on the previous studies, the model by Cai et al. (2000) was
173 applied for forestland, shrubland and grassland, and the method by Liu et al. (1999) was used
174 for dry land (Text S1). While for water, paddy field, garden plot, urban land and bare land,
175 values of 0, 0.1, 0.18, 0.01 and 0.7 were assigned, respectively (Cai et al., 2000; Yang et al.,
176 2003; Rao et al. 2014).

177 The P factor describes the impact of support practices. It is the ratio of soil loss with
178 contouring and strip cropping to that corresponding to losses under up-and-down-slope
179 farming (Wischmeier and Smith, 1978). The P factor values for agricultural land vary widely
180 in different regions because of different farming practices and geographical environments.
181 Based on the study of the Southern Hillside Area of China (Chen et al. 2014), we assigned
182 dry land, paddy field and garden plot with the values of 0.15, 0.4 and 0.18, respectively. For
183 other land use types, P factor values from these studies (Yang et al., 2003; Teng, 2017) were
184 applied.

185 **2.3.2 Parameters in the SDR model**

186 Threshold flow accumulation is used to extract streams from a DEM. The number of
187 upstream cells that must flow into a cell before it is considered part of a stream (Sharp et al.,
188 2018), was set to 1000 in this study similar to previous research (Zhong et al., 2013). The k_b
189 and IC_0 determine the shape of the relationship between SDR and IC (Sharp et al., 2015).
190 Vigiak et al. (2012) suggested that IC_0 is landscape independent and that the model is
191 sensitive to k_b . Therefore, we set IC_0 as the default value of 0.5 and adjusted k_b according to
192 the features of the study basin. The k_b was set as the value of 3.8 based on the previous
193 studies (Hamel et al., 2015; Hamel et al., 2017) and the model calibration tests.

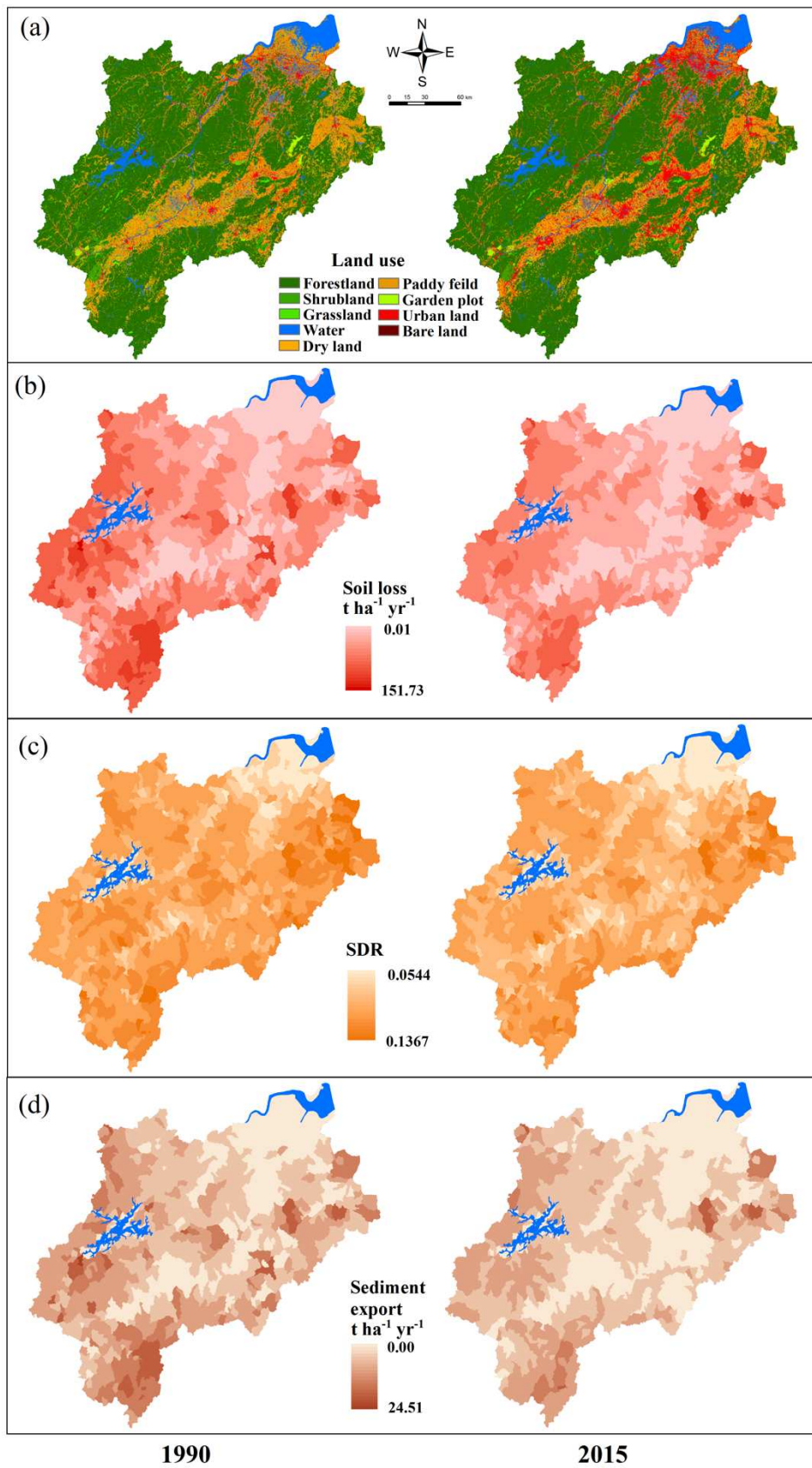
194 2.4 Validation

195 In this study, we validated the model results using the observation data and the previous
196 researchers (Table S2). The observation data for the Qiantang River Basin covers two
197 provinces, Anhui Province and Zhejiang Province, and thus we validated the results using
198 annual average values. First, the downward trend of soil loss in the published data since the
199 1960s was consistent with the trend in this study. Next, the average value of resulting SDR
200 was 0.1021 from 1990 to 2015, close to the published value of 0.11 from 1996 to 2005
201 (MWR, 2010a). The long-time average annual sediment yield in four gauging stations of
202 study basin, Quzhou, Lanxi, Shangyu and Zhuji, were recorded as 1.91 t ha⁻¹ yr⁻¹, 1.24 t ha⁻¹
203 yr⁻¹, 1.05 t ha⁻¹ yr⁻¹ and 0.98 t ha⁻¹ yr⁻¹, respectively, with an average value for the Qiantang
204 River Basin of 1.18 t ha⁻¹ yr⁻¹ (measured over 2.44 km²). The range of the resulting sediment
205 export values, from 1.69 t/ha in 1990 to 1.22 t ha⁻¹ yr⁻¹ in 2015, agreed well with the actual
206 value ranges. In addition, a good consistency of spatial distribution between the published
207 soil erosion regions of Zhejiang Province and the identified high-risk regions in the results
208 was found (Fig. S1). Thus, it was possible to confirm that the model and parameters used
209 here were able to reliably simulate general sediment export and the model results were
210 reasonable in the study basin.

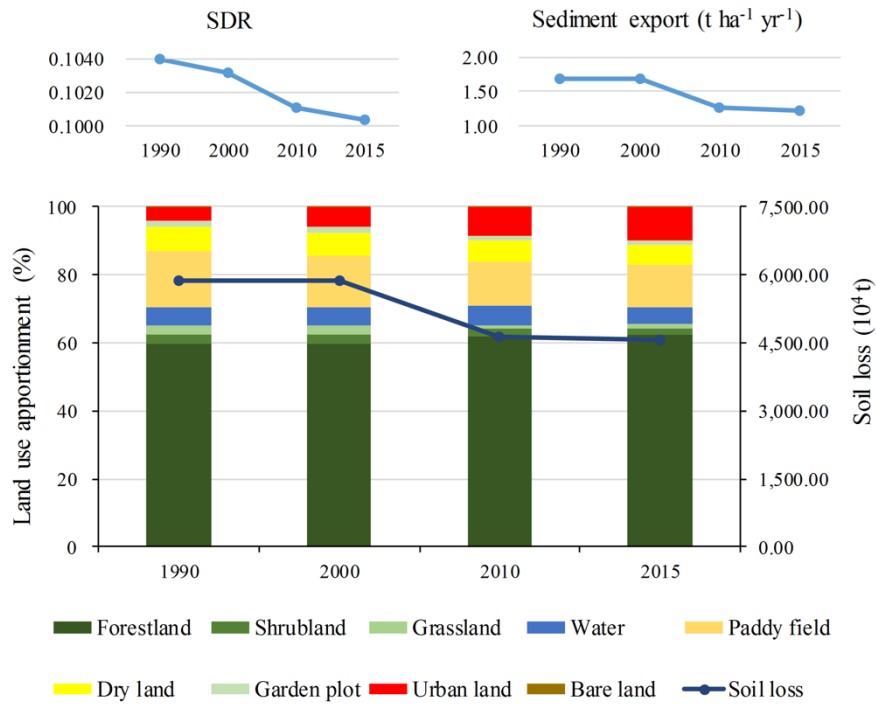
211 3 Results

212 3.1 Land use change from 1990 to 2015

213 Fig. 2(a) shows that land use has undergone dramatic changes, with the main conversion
214 of cropland to forestland and urban land from 1990 to 2015. The area of forestland accounted
215 for about 60% of the total area (Fig. 3) and increased from 25431.83 km² to 26608.41 km²,
216 and the area of urban land rapidly expanded from 4.01% to 10.08% and increased by 2587.89
217 km² during the study period (Table S3). Conversely, cropland (paddy field and dry land)
218 experienced a significant decline of 5.51%, including 1788.35 km² and 559.83 km² losses of
219 paddy field and dry land, respectively. Some 17.86% and 74.54% of cropland area loss were
220 converted to forestland and urban land (Table S4). Meanwhile, the areas of shrubland,
221 grassland, water, garden plot, and bare land moderately decreased. According to the change
222 area proportions in different periods, land use presented more drastic changes between 2000
223 and 2010 compared to the periods of 1990-2000 and 2010-2015 (Table S3). Spatially, land
224 use changes mainly occurred in the plain area, including the Hang-Jia-Hu Plain and the
225 Jin-Qu Basin (Fig. 2(a)).



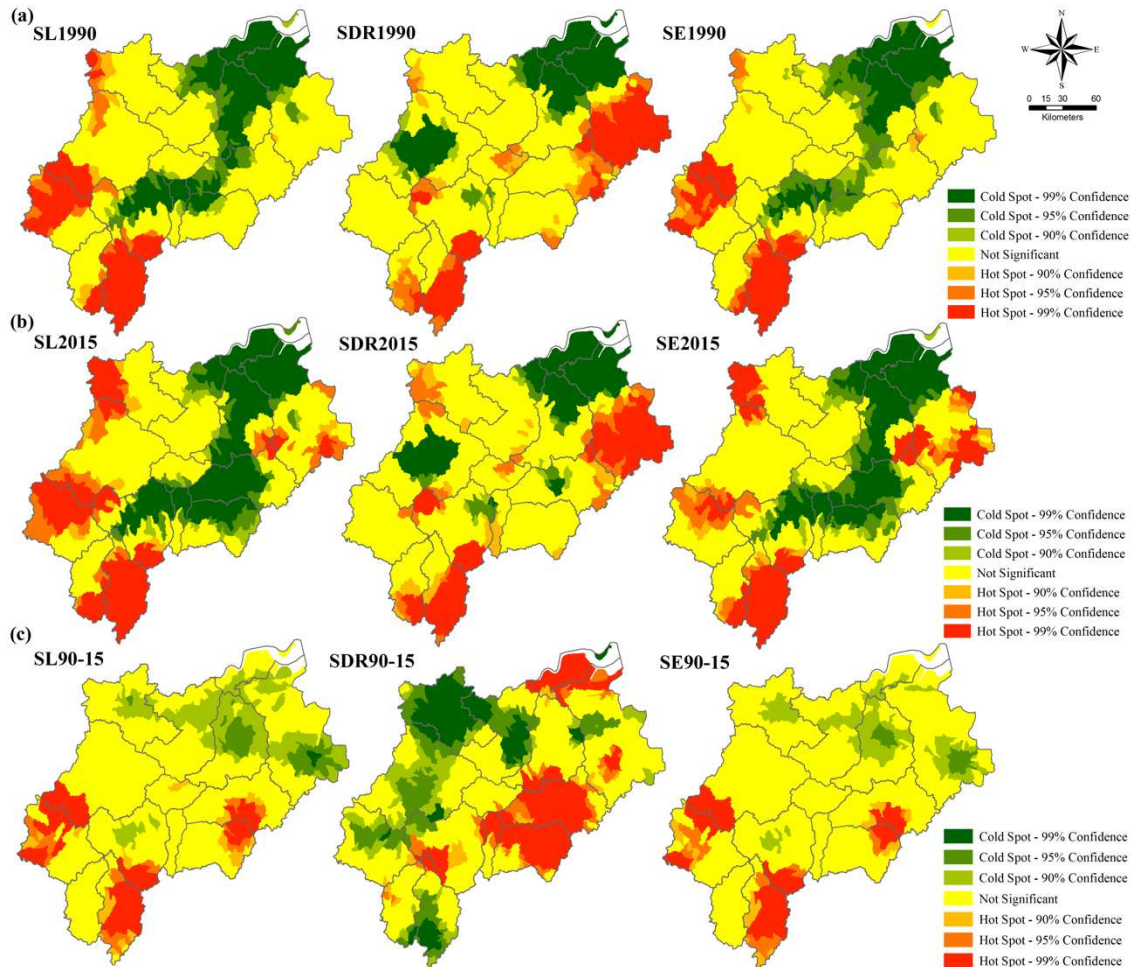
227 **Fig. 2.** Spatial distribution of (a) land use; the average values of (b) soil loss, (c) SDR and (d) sediment
 228 export, for each sub-watershed between 1990 and 2015.



229

230 **Fig. 3.** Land use composition and the changes in soil loss, SDR and sediment export from 1990 to 2015 in
 231 the study basin.

232



233

234 **Fig. 4.** Spatial distribution of hotspots and cold spots of soil loss (SL), SDR, and sediment export (SE) in
 235 (a) 1990 and (b) 2015, and (c) differences between the average values of 736 sub-watersheds in 1990 and
 236 these in 2015.

237 **3.2 Analysis of “land use change → changes in soil loss and SDR”**

238 **3.2.1 Changes in soil loss and SDR from 1990 to 2015**

239 The average soil loss decreased from $13.79 \text{ t ha}^{-1} \text{ yr}^{-1}$ in 1990 to $10.70 \text{ t ha}^{-1} \text{ yr}^{-1}$ in 2015.
 240 The total values of soil loss were $5880.24 \cdot 10^4 \text{ t}$, $5874.41 \cdot 10^4 \text{ t}$, $4642.09 \cdot 10^4 \text{ t}$ and
 241 $4563.66 \cdot 10^4 \text{ t}$ in 1990, 2000, 2010 and 2015, respectively (Table 1). The average soil loss
 242 from bare land was highest among all land use types and had the largest drop from 686.10 t
 243 $\text{ha}^{-1} \text{ yr}^{-1}$ in 1990 to $328.69 \text{ t ha}^{-1} \text{ yr}^{-1}$ in 2015. Meanwhile, because the area of bare land
 244 reduced from 120.38 km^2 to 14.58 km^2 , the total soil loss from bare land decreased by
 245 $778.01 \cdot 10^4 \text{ t}$. This decrease accounted for approximately 60% of the total decreased soil loss
 246 (Table 1). Some 68.76% of bare land was converted to forestland (Table S4) and this
 247 conversion resulted in a decrease of $700.83 \cdot 10^4 \text{ t}$ in soil loss. In addition, the soil loss from
 248 cropland and garden plot reduced by $255.21 \cdot 10^4 \text{ t}$ and $301.27 \cdot 10^4 \text{ t}$ (Table 1). Conversely,
 249 the total soil loss from forestland and urban land increased slightly by $99.24 \cdot 10^4 \text{ t}$ and

250 29.82*10⁴ t, and the average value of soil loss from urban land increased from 0.98 t ha⁻¹ yr⁻¹
 251 to 1.08 t ha⁻¹ yr⁻¹ (Table 1).

252 Using the Hot Spot Analysis (Getis-Ord Gi*) embedded in ArcGIS software, we found
 253 that hotspots of soil loss were mostly clustered in the hilly sub-watersheds in the Wuxi River
 254 watershed, the Majinxi River watershed and the Xin'an River watershed in 1990, and in the
 255 additional sub-watersheds in the Fenshui River watershed in 2015 (Fig. 4). In contrast, most
 256 cold spots were identified in flat terrains, such as the Hang-Jia-Hu Plain and Jin-Qu Basin,
 257 and spread to the peripheral sub-watersheds due to the conversion of cropland to urban land
 258 in the plain from 1990 to 2015. Soil loss had a pronounced decrease (hotspots) in the Wuxi
 259 River watershed, the junction of the Dongyang River watershed and Wuyi River watershed
 260 and the junction of the Majinxi River watershed and Xin'an River watershed from 1990 to
 261 2015 (Fig. 4(c)). Relatively, the cluster of the cold spots of soil loss change (where soil loss
 262 increased) was insignificant and distributed in the eastern sub-watersheds (Fig. 4(c)).

263 The SDR values in 1990, 2000, 2010 and 2015 were 0.1040, 0.1031, 0.1011 and 0.1003
 264 respectively across the whole basin (Fig. 3). The SDR of all land use types declined except
 265 for that of grassland (Fig. S2). The SDR for bare land was the highest and most stable, from
 266 0.1497 in 1990 to 0.1495 in 2015. In contrast, the SDR for urban land was the lowest and
 267 obviously reduced from 0.0820 in 1990 to 0.0798 in 2015 (Fig. S2). Spatially, the areas with
 268 the highest SDR were near rivers in the hills, and the areas with the lowest SDR were located
 269 in the large plains.

270 Fig. 4 indicates that the sub-watersheds with low SDR clustered in the Xin'an River
 271 watershed and Hang-Jia-Hu Plain in 1990 and 2015, and those with high SDR clustered in
 272 the upstream regions of the Cao'e River watershed and Wuxi River watershed (Fig. 4(a)(b)).
 273 Moreover, Fig. 4(c) shows that the sub-watersheds with a large decrease (hotspots) in SDR
 274 were found in the Qiantang River estuary, Dongyang River, Wuyi River and Jinhua River. In
 275 these areas, a considerable amount of cropland was occupied by urban land. Simultaneously,
 276 the cold spots were identified in the west of the basin, including the Fenshui River watershed,
 277 Xin'an River watershed and Wuxi River watershed.

278 **Table 1**

279 Average and total values of soil loss and sediment export for different land use types from 1990 to 2015 in
 280 the study area.

	Year	Forestland	Shrubland	Grassland	Paddy field	Dry land	Garden plot	Urban land	Bare land	A/T
ASL	1990	11.36	14.27	11.93	3.39	32.60	96.91	0.98	686.10	13.79
	2000	11.33	14.25	12.37	3.54	33.53	82.97	0.96	747.20	13.77
	2010	11.26	14.42	15.59	3.60	30.81	60.35	1.06	386.07	10.88

	2015	11.23	14.44	16.91	3.63	31.64	61.19	1.08	328.69	10.70
TSL	1990	2888.85	161.74	144.02	236.93	1008.47	597.58	16.72	825.94	5880.24
	2000	2894.00	161.85	131.51	224.71	960.73	639.57	23.53	838.51	5874.41
	2010	2972.44	132.29	84.24	201.84	827.95	310.33	38.83	74.20	4642.12
	2015	2988.09	118.33	76.28	188.62	801.57	296.31	46.54	47.93	4563.66
ASE	1990	1.17	1.55	1.38	0.44	4.73	13.25	0.09	105.73	1.69
	2000	1.17	1.54	1.42	0.46	4.86	11.36	0.09	115.05	1.69
	2010	1.15	1.54	1.80	0.47	4.50	8.75	0.10	58.25	1.26
	2015	1.15	1.54	1.94	0.47	4.60	8.77	0.10	50.18	1.22
TSE	1990	298.15	17.54	16.67	31.05	146.36	81.68	1.61	127.28	720.34
	2000	298.46	17.53	15.15	29.36	139.25	87.58	2.25	129.10	718.67
	2010	303.94	14.16	9.73	26.30	121.07	44.98	3.69	11.19	535.07
	2015	305.16	12.62	8.77	24.43	116.45	42.46	4.44	7.32	521.65

281 Note: ASL: average soil loss ($\text{t ha}^{-1} \text{ yr}^{-1}$); TSL: total soil loss (t); ASE: average sediment export ($\text{t ha}^{-1} \text{ yr}^{-1}$);
282 TSE: total sediment export (t); A/T: average value or total value.

283 3.2.2 Relationships between land use composition, soil loss and SDR

284 We analyzed the relationships in the 763 sub-watersheds between land use composition
285 and soil loss and between land use composition and SDR using Pearson's correlation analysis
286 (Table 2). The proportion of forestland was strongly and positively correlated with soil loss
287 and SDR. Conversely, the proportion of urban land was strongly and negatively correlated
288 with soil loss and SDR. There was a significantly negative correlation between the proportion
289 of water and SDR. The proportion of cropland had a strong and negative correlation with soil
290 loss (paddy field was stronger than dry land), in contrast to a weakly negative correlation
291 with SDR. The results revealed that soil loss was relatively low in sub-watersheds dominated
292 by urban land and cropland, and high in sub-watersheds with high proportions of bare land
293 and forestland. SDR was relatively low in sub-watersheds dominated by urban land and water
294 but was high in sub-watersheds with high areas of forestland.

295 **Table 2**

296 Pearson correlation coefficients for the relationship between land use proportion and the average values of
297 soil loss (SL) and SDR in 763 sub-watersheds from 1990 to 2015.

		Forestland	Shrubland	Grassland	Water	Paddy field	Dry land	Garden plot	Urban land	Bare land	Cropland
1990	SL	0.47**	0.14**	-0.13**	-0.32**	-0.47**	-0.22**	0.21**	-0.43**	0.55**	-0.43**
	SDR	0.41**	0.07	-0.01	-0.83**	-0.16**	0.05	0.20**	-0.46**	0.13**	-0.09*
2000	SL	0.47**	0.15**	-0.12**	-0.32**	-0.44**	-0.21**	0.17**	-0.43**	0.57**	-0.40**

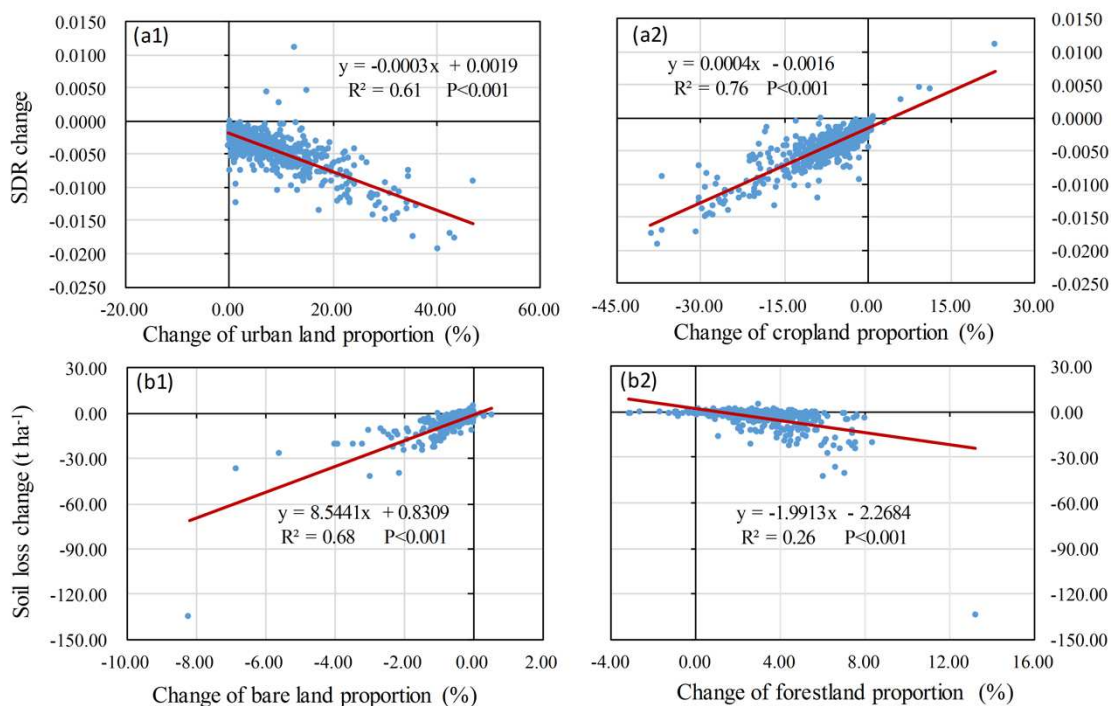
	SDR	0.47**	0.07*	-0.03	-0.81**	-0.13**	0.03	0.15**	-0.55**	0.12**	-0.08*
2010	SL	0.58**	0.08*	0.02	-0.37**	-0.44**	-0.22**	0.22**	-0.58**	0.12**	-0.41**
	SDR	0.50**	0.04	0.07	-0.78**	-0.11**	0.08*	0.11**	-0.58**	-0.01	-0.03
2015	SL	0.60**	0.07	0.04	-0.36**	-0.43**	-0.21**	0.21**	-0.61**	0.12**	-0.40*
	SDR	0.54**	0.05	0.07	-0.76**	-0.12**	0.05	0.10**	-0.60**	-0.01	-0.06

298 * P<0.05 (two-tailed)

299 ** P<0.01(two-tailed)

300 3.2.3 Relationships between changes in individual land use types and changes in soil loss 301 and SDR

302 Land use changes resulted in soil loss and SDR changes from 1990 to 2015. To further
303 quantify the contribution of changes in individual land use types, we examined the changes in
304 soil loss and SDR against changes in land use proportion (Fig. 5). Strong positive correlations
305 were found between changes in bare land and soil loss ($R^2=0.68$, $P<0.001$) and negative
306 correlations were found between changes in forestland and soil loss ($R^2=0.26$, $P<0.001$).
307 Conversely, there was no significant relationship between SDR change and forestland change
308 ($R=0.052$, $P=0.151$) (Fig. S3). SDR changes showed more significant correlations with
309 changes in land use more closely associated with human activities, such as cropland ($R^2=0.76$,
310 $P<0.001$) and urban land ($R^2=0.61$, $P<0.001$). A weak relationship was found between soil
311 loss and cropland changes ($R=-0.095$, $P=0.009$) (Fig. S4). As a result, soil loss decreased
312 sharply in sub-watersheds where bare land was converted to forest. Similarly, SDR also
313 showed a dramatic decline in sub-watersheds where cropland was converted to urban land.



314

315 Relationships between changes in the area proportion of different land use types and changes in the

Fig. 5.

316 average values of soil loss and SDR in the sub-watersheds: (a1) SDR vs urban land; (a2) SDR vs cropland;
317 (b1) soil loss vs bare land; (b2) soil loss vs forestland.

318 **3.3 Analysis of “changes in soil loss and SDR → sediment export change”**

319 **3.3.1 Sediment export change from 1990 to 2015**

320 Sediment export had a significant decline from 1990 to 2015 (Fig. 2). The average
321 sediment export decreased from $1.69 \text{ t ha}^{-1} \text{ yr}^{-1}$ to $1.22 \text{ t ha}^{-1} \text{ yr}^{-1}$, and the total sediment
322 export reduced from $720.34 \times 10^4 \text{ t}$ to $521.65 \times 10^4 \text{ t}$, with approximately 60% of this decline
323 from the loss of bare land (Table 1). The top three reductions in sediment export caused by
324 land use transitions were the conversions of bare land to forestland, garden plot to forestland
325 and dry land to forestland. These accounted for 54.58%, 19.18% and 14.72% of the total
326 decrease, respectively (Table S5). Conversely, the top three increases in sediment export were
327 $17.27 \times 10^4 \text{ t}$, $11.17 \times 10^4 \text{ t}$ and $4.00 \times 10^4 \text{ t}$, as a result of conversions of paddy field to dry land,
328 grassland to dry land and paddy field to garden plot, respectively (Table S5). The results
329 implied that decreases in bare land greatly contributed to the reductions of sediment export.
330 In contrast, increases in agricultural land, such as cropland and garden plot, were found to
331 increase sediment export in the study basin.

332 Spatially, the cold spots of sediment export were clustered in the low-slope areas and the
333 cold spots and hotspots in 2015 were more widely spread than those in 1990 (Fig. 4(a) (b)).
334 The Wuxi River watershed was found to contain most hotspots of sediment export in 1990
335 and in 2015, as well as most hotspots of sediment export change from 1990 to 2015. That is,
336 this watershed dramatically declined while having high sediment export. In addition, there
337 were some hotspots of sediment export in the Fenshui River watershed, the junction of the
338 Xin'an River watershed and Majinxi River watershed, and Cao'e River watershed (Fig. 4(a)
339 (b)). Rather, the cluster of the cold spots of sediment export change was relatively
340 insignificant (Fig. 4(c)).

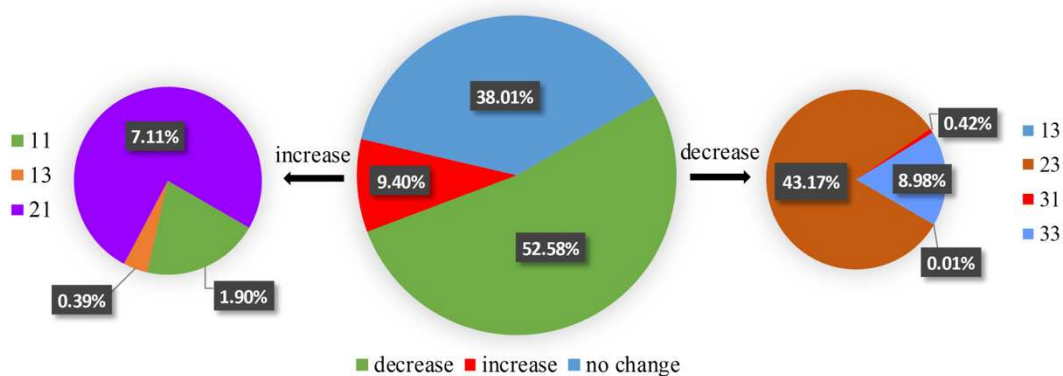
341 **3.3.2 Effects of changes in soil loss and SDR on sediment export change**

342 From 1990 to 2015, increases and decreases of soil loss accounted for 2.43% and 9.83%
343 respectively of the whole watershed area and the increases and decreases of SDR accounted
344 for 10.26% and 55.21% (Fig. 2). The area of increased sediment export accounted for 9.40%
345 of the whole watershed area, mainly due to 7.11% of the total area where SDR increased and
346 soil loss was unchanged. The area of decreased sediment export accounted for 52.58% of the
347 whole watershed area, due to 43.17% of the total area where SDR decreased and soil loss was
348 unchanged (Fig. 6). That is, SDR change resulted in a large-scale change in sediment export
349 in the study area.

350 Alternately, the reduction in the average value of soil loss (22.41%) was much greater
351 than that of SDR (3.56%) and the average value of sediment export reduced by 27.81%. Fig.
352 4 shows that the distributions in hotspots (high values) and cold spots (low values) of
353 sediment export and sediment export change were highly consistent with those of soil loss.

354 Generally, soil loss change resulted in a significant decrease in the total sediment export and
 355 related to the magnitude of the values of sediment export change in the sub-watersheds.

356 Overlay analysis showed that there were low values of soil loss, SDR and sediment
 357 export in the Hang-Jia-Hu Plain in 1990 and 2015, while high values were found in the Wuxi
 358 River watershed and the downstream regions of the Qu River watershed and Jiangshangang
 359 River watershed (Fig. 4(a) (b)). Significant decreases (hotspots) in soil loss, SDR and
 360 sediment export were found at the junction of the Dongyang River watershed and Wuyi River
 361 watershed (Fig. 4(c)).



362
 363 **Fig. 6.** The area proportions of sediment export changes and their compositions from 1990 to 2015. The
 364 values of 1, 2 and 3 represent increases, no change and decreases from 1990 to 2015, respectively. The first
 365 of the ten digits in the legends represents the change in soil loss, and the second represents the change in
 366 SDR.

367 4 Discussion

368 4.1 Evaluation on sediment export in the Qiantang River Basin

369 This study highlighted the “three-level” relationships throughout the process of sediment
 370 transport dynamics, and distinguished the different effects of sediment source and sediment
 371 delivery on sediment export reduction under the rapid land use change in the Qiantang River
 372 Basin. Urbanization and afforestation, which were in accordance with the land use policies,
 373 were found to be the dominant causes of reduction in SDR and soil loss, respectively, and
 374 greatly encouraged a decrease in sediment export. This finding was consistent with some
 375 similar studies, which also showed a decline in sediment yield due to land use change and
 376 soil conservation projects (Chu et al., 2009; Liu et al., 2013). Reduced sediment yield from
 377 major rivers in China was found and its main driving factor was converted from dam
 378 construction to conservation measures (especially the Grain for Green Program) after 1999
 379 (Li et al., 2018). Since the 1950s, sediment loads from rivers in South China, including the
 380 Pearl River, Min River and Qiantang River, reduced by 44%~58% (Hu et al., 2010). Among
 381 the three rivers, the Qiantang River had the least soil loss and SDR, but its soil loss was far
 382 more than the soil loss tolerance in China (2~10 t ha⁻¹ yr⁻¹) (MWR, 2010a). In addition, main

383 anthropogenic drivers of the decreased sediment loads from these rivers were different since
384 the 1990s. ~90% of reduction in the Pearl River Basin was caused by dam construction (Wu
385 et al., 2012). A clear decrease in sediment transport in the Min River could be attributed to
386 reservoir construction and sand mining (Liu et al., 2008; Hu et al., 2010). However, reduction
387 in the Qiantang River Basin primarily benefited from soil conservation practices, especially
388 the increased forestland (Zhang et al., 2015).

389 **4.2 Drivers of land use change from 1990 to 2015**

390 In this study, the main land use changes were the conversion of cropland to forestland and
391 urban land, and presented different change rates in three periods from 1990 to 2000, 2000 to
392 2010 and 2010 to 2015, which can be described as a process of “start-acceleration-slow”
393 (Table S3). Land use dynamics have been primarily driven by economic development and
394 land use policies in China (Liu et al., 2014). In the first decade, because the socialist market
395 economic system launched in 1992, urbanization was comprehensively promoted and the
396 Afforestation and Greening Project was on highlight era stage, land use change was in the
397 “start” stage. In the next decade, land use change accelerated with a rate of 8.01% (Table S3)
398 and the proportions of forestland and urban land greatly increased due to accelerating
399 urbanization and ecological restoration projects. In recent years, as the Farmland Protection
400 System was constantly revised and comprehensively implemented, the transformation of
401 agricultural land to non-agricultural land gradually reduced, the growth of forestland from
402 cropland slowed but urbanization continued at the same rate. Under these land use change
403 patterns, this study found a reduction in sediment source and delivery, resulting in a decline
404 in sediment export. However, as the Permanent Prime Farmland Protection Policy and other
405 Farmland Protection policies are implemented, resulting in different patterns of land use
406 change, it may difficult to predict future sediment export.

407 **4.3 Discussion on the “three-level” relationships**

408 The links between land use change, soil loss and SDR are built on the C and P factors.
409 Variation in the values and spatial distribution of C factor directly alters the soil loss, and the
410 reductions of C factor result in decreases in IC related to SDR values. The P factor has an
411 impact on soil loss but has no direct correlation with SDR, with smaller C and P factors
412 related to stronger controlling sediment export (Table 3).

413 The distributions of different land use types follow a number of general trends: forestland
414 tends to be found in the hilly and steep areas, cropland and urban land are typically found in
415 in the plain areas. Sun et al. (2014) noted that the hilly and gully regions with higher LS
416 values are topographically prone to erosion, which largely explains the relationship between
417 soil loss and land use (Table 2) and distribution of the cold spots and hotspots of soil loss (Fig.
418 4). In addition, bare land with high value of C factor and that tends to be found in areas with
419 terrible topographic and soil environments, was associated with much large soil losses in the
420 sub-watersheds than losses from other land use types (Table 1). As a result, changes in bare
421 land resulted in large fluctuations of soil loss in the sub-watersheds (Fig. 5(b1)). Increases in
422 forestland were comparatively small because of the original dominant forestland proportion

423 (Fig. 1). As a result, reduction in soil loss from increased forestland was not as remarkable as
424 that from decreased bare land in the sub-watersheds (Fig. 5(b2)). Because the SDR of water
425 was the value of 0, sub-watersheds with larger proportion of water had lower SDR, such as
426 Xin'an River watershed. According to the study by Borselli et al. (2008), SDR depends on
427 the index of connectivity calculated from C factor, slope, and contribution area as well as
428 flow path. Both urban land and cropland near rivers had short flow paths and low slope
429 values, but lower SDR in urban land and higher SDR in cropland were found that were
430 caused by the large differences in C factor (Fig. S2). Thus, the proportion of cropland had a
431 less negative correlation with SDR than urban land in the sub-watersheds (Table 2).
432 Large-scale agricultural planting may result in a much better connectivity caused by a
433 degraded landscape, surface stoniness and raiding channels in the stream network (Beguería
434 et al., 2005). Further, the study by Alatorre et al. (2012) also showed an 84% increase in SDR
435 when the study area was occupied by annual crops compared with no crops, implying the
436 close positive correlation between SDR and cropland (Fig. 5(a2)). It was proved that the
437 upstream regions of Cao'e River with developed agriculture surrounded by mountains had a
438 high SDR. Urban environments have a very low connectivity because of their low slopes and
439 artificial surface providing a stronger barrier to sediment transport than other land use types
440 (Borselli et al., 2008, Sharp et al., 2015). Therefore, watersheds with increased urban land
441 from cropland, such as Qiantang River Estuary, made a great contribution to the decrease in
442 SDR (Fig. 5(a1)).

443 SDR was found to be more stable in the large basin than soil loss when the effects of soil
444 loss and SDR on sediment export are compared. SDR can be affected by the peripheral land
445 use change in a given area contributing to the spatial connectivity of IC, therefore, the impact
446 from it is related to the spatial scale of sediment export change. However, soil loss, as the
447 main sediment source, is limited by the scope of land use change and fluctuates with land
448 use/cover change. Therefore, its influence controls the total value of sediment export to
449 rivers.

450 **4.4 Suggestions**

451 Significant progress and improvement have been made in sediment retention services
452 with the development of soil and water conservation projects and land policies in Zhejiang
453 (MWR, 2010b). The government invested 45.80 million Yuan to support the National Soil
454 and Water Conservation Key Project in Zhejiang, including regulating slope drainage systems,
455 afforestation on hills and converting sloping fields into terraces, by the Zhejiang Bulletin of
456 Soil and Water Conservation (2015). Effective engineering and biological measures are
457 important for sediment export control (Lin et al., 2008; Feng et al., 2010). Boix-Fayos et al.
458 (2008) also suggested that land use changes can have important long-term effects on
459 sediment yield with no side-effects. Therefore, it is also important to define comprehensive
460 land use plans as well. Based on the results of this study, two land use types, forestland and
461 bare land, can be used to control the sediment sources. It is important to improve vegetation
462 coverage and quality, protecting the ecological forestland and greening bare land.
463 Alternatively, the strong correlation between SDR change and changes in cropland and urban

land suggests additional ways to control the sediment delivery. As the Farmland Protection Policy, means that reducing SDR by converting cropland to urban land and forestland is impractical, we draw lessons from recent land development policies and identify potentially beneficial measures. These included turning dry land to paddy fields and building ecological villages and towns in low-slope hilly regions. Additionally, there are opportunities for environment treatments to benefit areas with high SDR that are located near rivers in the hilly environments. According to the hotspot analysis, as the overlay areas of high values of soil loss, SDR and sediment export, the Wuxi River watershed should be listed as the key areas for future treatment. At the same time, these areas have large potential in improving sediment retention (Fig. 4(c)). However, the Hang-Jia-Hu Plain could be considered as a low-risk area. In the future, land use should be optimized in the upstream regions with severe sediment export, and more soil and water conservation projects implemented in those areas near rivers.

Table 3

Average values of C factor, P factor, CP and IC from 1990 to 2015 in the study basin.

	1990	2000	2010	2015
C	0.0559	0.0531	0.0473	0.0449
P	0.6218	0.6361	0.6548	0.6652
CP	0.0231	0.0225	0.0195	0.0188
IC	-6.7752	-6.8138	-6.8997	-6.9302

5 Conclusions

This study provided an effective method to evaluate sediment yield in a large basin. Based on the analysis of the “three-level” relationships, we explored the reduced sediment export (from 1.69 t ha⁻¹ yr⁻¹ in 1990 to 1.22 t ha⁻¹ yr⁻¹ in 2015) from the two perspectives of the decreased sediment source and a weakened sediment delivery function, using InVEST SDR model in the Qiantang River Basin. Urbanization and afforestation made the main contributions to decreases in soil loss and SDR, respectively. Furthermore, soil loss change and SDR change had strong effects on the magnitude of the value and the spatial scale of the sediment export change, respectively. In order to cope with new patterns of land use change, driven by continuous urban expansion, strict farmland protection policies and ecological protection projects in the future, this study identified a number of practical suggestions related to land use policies (e.g. building ecological villages and towns in low-slope hilly regions, turning dry land to paddy fields and implementing ecological forest protection) to improve the sediment management and aquatic ecosystems in the study basin.

However, some limitations were also highlighted here for guiding future studies. Predicting sediment yield remains challenging even for state-of-the-art models since sediment sources are diverse. In this study, the RUSLE model was used to measure the main sediment source from water erosion and thus the contribution from additional sediment sources might not be taken into account in the results. That is to say, this method is defective to be applied in some basins where are dominant by other sediment sources, such as mass erosion. What’s more, predicting sediment yield may be impacted by the DEM quality

499 (resolution). Further analysis is needed to explore the sensitivity of sediment yield to DEM
500 with a complicated topography in the Qiantang River Basin.

501 **Acknowledgments**

502 This research was supported by the Zhejiang Provincial Natural Science Foundation of
503 China (No. LY18G030006), the National Natural Science Foundation of China (No.
504 41701171) and the ZJU-Leeds Partnership Fund.

505 **Author Contributions**

506 Mengmeng Zhou, Jinsong Deng, Yi Lin and Ke Wang conceived and designed this study;
507 Marye Belete, Lingyan Huang and Muye Gan collected data; Mengmeng Zhou analyzed data
508 and wrote this paper; Alexis Comber and Jinsong Deng revised the manuscript; all authors
509 read and approved the final manuscript.

510 **Appendix A. Supplementary data**

511 Supplementary data associated with this article can be found in the online version. Text
512 S1, Table S1–5 and Figure S1–4.

513 **References**

- 514 Alatorre, L.C., Begueria, S., Lana-Renault, N., Navas, A., Garcia-Ruiz, J.M., 2012. Soil erosion and sediment
515 delivery in a mountain catchment under scenarios of land use change using a spatially distributed
516 numerical model. *Hydrol. Earth Syst. Sci.* 16, 1321–1334. <https://doi.org/10.5194/hess-16-1321-2012>
- 517 Bakker, M.M., Govers, G., Doorn, A. Van, Quetier, F., Chouvardas, D., Rounsevell, M., 2008. The response of
518 soil erosion and sediment export to land-use change in four areas of Europe : The importance of landscape
519 pattern. *Geomorphology.* 98, 213–226. <https://doi.org/10.1016/j.geomorph.2006.12.027>
- 520 Beguería, S., López-Moreno, J.I., Gómez-Villar, A., Rubio, V., Lana-Renault, N., and García-Ruiz, J. M., 2005.
521 Fluvial adjustments to soil erosion and plant cover changes in the Central Spanish Pyrenees, *Geografiska*
522 *Annaler*, 88A, 177–186. <https://doi.org/10.1111/j.1468-0459.2006.00293.x>
- 523 Borselli, L., Cassi, P., Torri, D., 2008. Prolegomena to sediment and flow connectivity in the landscape: A GIS
524 and field numerical assessment. *Catena* 75, 268–277. <https://doi.org/10.1016/j.catena.2008.07.006>
- 525 Boix-Fayos, C., de Vente, J., Martínez-Mena, M., Barberá, G.G., Castillo, V., 2008. The impact of land use
526 change and check-dams on catchment sediment yield. *Hydrol. Process.* 22, 4922–4935.
527 <http://dx.doi.org/10.1002/hyp.7115>
- 528 Cai, C.F., Ding, S.W., Shi, Z.H., Huang, L., Zhang, G.Y., 2000. Study of applying USLE and geographical
529 information system IDRISI to predict soil erosion in small watershed. *J. Soil Water Conserv.* 14, 19–24 (in
530 Chinese). <http://dx.doi.org/10.3321/j.issn:1009-2242.2000.02.005>

- 531 Chen, S.X., Yuan, X.H., Xiao, L.L., Cai, H.Y., 2014. Study of Soil Erosion in the Southern Hillside Area of
 532 China Based on RUSLE Model. *Resour Sci.* 36(6), 1288-1297 (in Chinese).
 533 <http://kns.cnki.net/kcms/detail/detail.aspx?DBCode=CJFD&DBName=CJFD2014&fileName=ZRZY2014>
 534 06022
- 535 Chu, Z.X., Zhai, S.K., Lu, X.X., Liu, J.P., Xu, J.X., Xu, K.H., 2009. A quantitative assessment of human impacts
 536 on decrease in sediment flux from major Chinese rivers entering the western Pacific Ocean. *Geophys. Res.*
 537 *Lett.* 36, L19603. <https://doi.org/10.1029/2009GL039513>
- 538 Erskine, W.D., Mahmoudzadeh, A., Myers, C., 2002. Land use effects on sediment yields and soil loss rates in
 539 small basins of Triassic sandstone near Sydney, NSW, Australia. *Catena* 49, 271–287.
 540 [https://doi.org/10.1016/S0341-8162\(02\)00065-6](https://doi.org/10.1016/S0341-8162(02)00065-6)
- 541 Fang, H., 2017. Impact of land use change and dam construction on soil erosion and sediment yield in the black
 542 soil region , Northeastern China. *Land Degrad. Develop.* 28, 1482–1492.
 543 <http://dx.doi.org/10.1002/ldr.2677>
- 544 Feng, X., Wang, Y., Chen, L., Fu, B., Bai, G., 2010. Geomorphology Modeling soil erosion and its response to
 545 land-use change in hilly catchments of the Chinese Loess Plateau. *Geomorphology.* 118, 239–248.
 546 <https://doi.org/10.1016/j.geomorph.2010.01.004>
- 547 Fiener, P., Auerswald, K., Van Oost, K., 2011. Spatio-temporal patterns in land use and management affecting
 548 surface runoff response of agricultural catchments—A review. *Earth-Science Rev.* 106, 92–104.
 549 <https://doi.org/10.1016/j.earscirev.2011.01.004>
- 550 Hamel, P., Chaplin-Kramer, R., Sim, S., Mueller, C., 2015. A new approach to modeling the sediment retention
 551 service (InVEST 3.0): Case study of the Cape Fear catchment, North Carolina, USA. *Sci. Total Environ.*
 552 524–525, 166–177. <https://doi.org/10.1016/j.scitotenv.2015.04.027>
- 553 Hamel, P., Falinski, K., Sharp, R., Auerbach, D.A., Sánchez-Canales, M., Denny-Frank, P.J., 2017. Sediment
 554 delivery modeling in practice: Comparing the effects of watershed characteristics and data resolution
 555 across hydroclimatic regions. *Sci. Total Environ.* 580, 1381–1388.
 556 <https://doi.org/10.1016/j.scitotenv.2016.12.103>
- 557 Hu, C.H., Wang, Y.G., Zhang, Y.Q., Shi, H.L., 2010. Variation tendency of runoff and sediment load in China
 558 major rivers and its causes. *Adv Water Sci.* 21(4), 524-532 (in Chinese).
 559 <https://doi.org/10.14042/j.cnki.32.1309.2010.04.009>
- 560 Jiang, C., Li, D., Wang, D., Zhang, L., 2016. Quantification and assessment of changes in ecosystem service in
 561 the Three-River Headwaters Region, China as a result of climate variability and land cover change. *Ecol.*
 562 *Indic.* 66, 199–211. <https://doi.org/10.1016/j.ecolind.2016.01.051>
- 563 Keeler, B.L., Polasky, S., Brauman, K.A., Johnson, K.A., Finlay, J.C., O'Neill, A., Dalzell, B., 2012. Linking
 564 water quality and well-being for improved assessment and valuation of ecosystem services. *Proc. Natl.*
 565 *Acad. Sci.* 109 (45), 18619–18624. <https://doi.org/10.1073/pnas.1215991109>

- 566 Kondolf, G.M., Gao, Y., Annandale, G.W., Morris, G.L., Jiang, E., Zhang, J., Cao, Y., Carling, P., Fu, K., Guo,
567 Q., Hotchkiss, R., Peteuil, C., Sumi, T., Wang, H.-W., Wang, Z., Wei, Z., Wu, B., Wu, C., Yang, C.T.,
568 2014. Sustainable sediment management in reservoirs and regulated rivers: Experiences from five
569 continents. *Earth's Futur.* 2, 256–280. <http://dx.doi.org/10.1002/2013EF000184>
- 570 Kong, L.Q., Zheng, H., Rao E., Xiao, Y., Ouyang, Z., Li, C., 2018. Evaluating indirect and direct effects of
571 eco-restoration policy on soil conservation service in Yangtze River Basin. *Sci. Total Environ.* 631-632,
572 887-894. <https://doi.org/10.1016/j.scitotenv.2018.03.117>
- 573 Li, Z.G., Liu B.Z., 2006. Calculation on soil erosion amount of main river basin in China. *Sci Soil Water*
574 *Conserv.* 4 (2), 1-6 (in Chinese). <http://dx.doi.org/10.16843/j.sswc.2006.02.001>
- 575 Li, T., Wang, S., Liu, Y.X., Fu, Bo.J., 2018. Driving forces and their contribution to the recent decrease in
576 sediment flux to ocean of major rivers in China. *Sci. Total Environ.* 634, 534-541.
577 <https://doi.org/10.1016/j.scitotenv.2018.04.007>
- 578 Lin, W., Tsai, J., Lin, C., Huang, P., 2008. Assessing reforestation placement and benefit for erosion control: A
579 case study on the Chi-Jia-Wan Stream, Taiwan. *Ecol Model.* 211(3-4), 444–452.
580 <https://doi.org/10.1016/j.ecolmodel.2007.09.025>
- 581 Liu, B.Z., Liu, S.H., Zheng, S.D., 1999. Soil conservation and coefficient of soil conservation of crops. *Res. Soil*
582 *Water Conserv.* 6(2), 32–36 (in Chinese).
583 <http://kns.cnki.net/kcms/detail/detail.aspx?DBCCode=CJFD&DBName=CJFD9899&fileName=STBY902.0>
584 07
- 585 Liu, C., Sui, J., Wang, Z.Y., 2008. Sediment load reduction in Chinese rivers. *Int. J. Sed. Res.* 23, 44–55.
586 [https://doi.org/10.1016/S1001-6279\(08\)60004-9](https://doi.org/10.1016/S1001-6279(08)60004-9)
- 587 Liu, C., Sui, J., He, Y., Hirshfield, F., 2013. Changes in runoff and sediment load from major Chinese rivers to
588 the Pacific Ocean over the period 1955–2010. *Int. J. Sediment Res.* 28, 486–495.
589 [https://doi.org/10.1016/S1001-6279\(14\)60007-X](https://doi.org/10.1016/S1001-6279(14)60007-X)
- 590 Liu, J., Kuang, W., Zhang, Z., Xu, X., Qin, Y., Ning, J., Zhou, W., Zhang, S., Li, R., Yan, C., Wu, S., Shi, X.,
591 Jiang, N., Yu, D., Pan, X., Chi, W., 2014. Spatiotemporal characteristics, patterns and causes of land use
592 changes in China since the late 1980s. *Acta Geogr. Sin.* 69, 3–14 (in Chinese).
593 <https://doi.org/10.11821/dlxb201401001>
- 594 Liu, J., Ning, J., Kuang, W., Xu, X., Zhang, S., Yan, C., Li, R., Wu, S., Hu, Y., Du, G., Chi, W., Pan, T., Ning, J.,
595 2018. Spatio-temporal patterns and characteristics of land-use change in China during 2010-2015. *Acta*
596 *Geogr. Sin.* 73, 789–802 (in Chinese). <https://doi.org/10.11821/dlxb201805001>
- 597 Lu, D., Li, G., Valladares, G.S., Batistella, A.M., 2004. Mapping soil erosion risk in rondonia, brazilian amazonia:
598 using rusle, remote sensing and gis. *L. Degrad. Dev.* 15, 499–512. <https://doi.org/10.1002/ldr.634>
- 599 Lu, H., Moran, C.J., Prosser, I.P., 2006. Modelling sediment delivery ratio over the Murray Darling Basin.

- 600 Environ. Model. Softw. 21, 1297–1308. <https://doi.org/10.1016/j.envsoft.2005.04.021>
- 601 McCool, D., et al., 1997. Slope-length and steepness factors (LS). In: Predicting Soil Ero-sion by Water: A
602 Guide to Conservation Planning with the Revised Universal SoilLoss Equation (RUSLE).
603 USDA-Agriculture Handbook No. 703, Chapter 4.
- 604 Ministry of Water Resources of China (MWR), Chinese Academy of Sciences (CAS), Chinese Academy of
605 Engineering (CAE), 2010a. Control of soil erosion and ecological security in China: soil erosion data
606 volume. Control of Soil Erosion and Ecological Security in China.Science Press, Beijing (in Chinese).
- 607 Ministry of Water Resources of China (MWR), Chinese Academy of Sciences (CAS), Chinese Academy of
608 Engineering (CAE), 2010b. Control of soil erosion and ecological security in China: Red Soil Region of
609 Southern China volume. Control of Soil Erosion and Ecological Security in China.Science Press, Beijing
610 (in Chinese).
- 611 Rao, E., Ouyang, Z., Yu, X., Xiao, Y., 2014. Spatial patterns and impacts of soil conservation service in China.
612 *Geomorphology* 207, 64–70. <https://doi.org/10.1016/j.geomorph.2013.10.027>
- 613 Rao, E., Xiao, Y., Ouyang, Z., Zheng, H., 2016. Changes in ecosystem service of soil conservation between
614 2000 and 2010 and its driving factors in southwestern China. *Chinese Geogr. Sci.* 26(2), 165–173.
615 <https://doi.org/10.1007/s11769-015-0759-9>
- 616 Renard, K.G., Foster, G.R., Weesies, G.A., McCool, D.K., Yoder, D.C., 1997. Predicting Soil Erosion by Water:
617 A Guide to Conservation Planning with the Revised Universal Soil Loss Equation (RUSLE) (Agricultural
618 Handbook No.703). US Department of Agriculture, Washington, DC.
- 619 Romano, G., Abdelwahab, O.M.M., Gentile, F., 2018. Catena Modeling land use changes and their impact on
620 sediment load in a Mediterranean watershed. *Catena* 163, 342–353.
621 <https://doi.org/10.1016/j.catena.2017.12.039>
- 622 Sánchez-Canales, M., López-Benito, A., Acuña, V., Ziv, G., Hamel, P., Chaplin-Kramer, R., Elorza, F.J., 2015.
623 Sensitivity analysis of a sediment dynamics model applied in a Mediterranean river basin: Global change
624 and management implications. *Sci. Total Environ.* 502, 602–610.
625 <https://doi.org/10.1016/j.scitotenv.2014.09.074>
- 626 Sheng, L., Jin, Y., Huang, J.F., 2010. Value estimation of conserving water and soil of ecosystem in China. *J.*
627 *Nat. Resour.* 25, 1105–1113 (in Chinese). <https://doi.org/10.11849/zrzyxb.2010.07.006>
- 628 Sharp, et al., 2018 InVEST User’s Guide. Available at:
629 <http://releases.naturalcapitalproject.org/invest-userguide/latest/>
- 630 Shi, Z.H., Ai, L., Fang, N.F., Zhu, H.D., 2012. Modeling the impacts of integrated small watershed management
631 on soil erosion and sediment delivery : A case study in the Three Gorges Area , China. *J. Hydrol.* 438–439,
632 156–167. <https://doi.org/10.1016/j.jhydrol.2012.03.016>

- 633 Sun, W., Shao, Q., Liu, J., Zhai, J., 2014. Assessing the effects of land use and topography on soil erosion on the
634 Loess Plateau in China. *Catena* 121, 151–163. <https://doi.org/10.1016/j.catena.2014.05.009>
- 635 Tang, L., Yang, D., Hu, H., Gao, B., 2011. Detecting the effect of land-use change on streamflow, sediment and
636 nutrient losses by distributed hydrological simulation. *J. Hydrol.* 409, 172–182.
637 <https://doi.org/10.1016/j.jhydrol.2011.08.015>
- 638 Tarboton, D., 1997. A new method for the determination of flow directions and upslope areas in grid digital
639 elevation models. *Water Resour. Res.* 33, 309–319. <https://doi.org/10.1029/96WR03137>
- 640 Teng, H.F., 2017. Assimilating Multi-source Data to Model and Map Potential Soil Loss in China.(PhD thesis).
641 Zhejiang University at Hangzhou, China.
642 <http://kns.cnki.net/kcms/detail/detail.aspx?DBCode=CDFD&DBName=CDFDLAST2017&fileName=1017071521.nh>
643
- 644 Vanacker, V., Govers, G., Barros, S., Poesen, J., Deckers, J., 2003. The effect of short-term socio-economic and
645 demographic change on landuse dynamics and its corresponding geomorphic response with relation to
646 water erosion in a tropical mountainous catchment, Ecuador. *Landscape Ecol.* 18, 1–15.
647 <https://doi.org/10.1023/A:1022902914221>
- 648 Van Rompaey, A.J.J., Verstraeten, G., Van Oost, K., Govers, G., Poesen, J., 2001. Modelling mean annual
649 sediment yield using a distributed approach. *Earth Surf Process. Landforms.* 26, 1221–1236.
650 <https://doi.org/10.1002/esp.275>
- 651 Vigiak, O., Borselli, L., Newham, L.T.H., McInnes, J., Roberts, A.M., 2012. Comparison of conceptual
652 landscape metrics to define hillslope-scale sediment delivery ratio. *Geomorphology.* 138, 74–88.
653 <https://doi.org/10.1016/j.geomorph.2011.08.026>
- 654 Walling, D.E., Fang, D., 2003. Recent trends in the suspended sediment loads of the world's rivers. *Glob. Planet.*
655 *Change* 39, 111–126. [https://doi.org/10.1016/S0921-8181\(03\)00020-1](https://doi.org/10.1016/S0921-8181(03)00020-1)
- 656 Wang, S., Fu, B., Piao, S., Lü, Y., Ciais, P., Feng, X., Wang, Y., 2016. Reduced sediment transport in the
657 Yellow River due to anthropogenic changes. *Nat. Geosci.* 9, 38–41. <https://doi.org/10.1038/ngeo2602>
- 658 Wang, X.K., Ouyang, Z.Y., Xiao, H., Miao, H., Fu, B.J., 2001. Distribution and division of sensitivity to
659 water-caused soil loss in China. *Acta Ecol. Sin.* 21, 14–19 (in Chinese).
660 <https://doi.org/10.3321/j.issn:1000-0933.2001.01.003>
- 661 Wei, W., Chen, L., Fu, B., Huang, Z., Wu, D., Gui, L., 2007. The effect of land uses and rainfall regimes on
662 runoff and soil erosion in the semi-arid loess hilly area, China. *J. Hydrol.* 335, 247–258.
663 <https://doi.org/10.1016/j.jhydrol.2006.11.016>
- 664 Williams, J.R., Jones, C.A., Dyke, P.T., A modelling approach to determining the relationship between erosion
665 and soil productivity. *Trans ASAE.* 27(1), 129–144. <https://doi.org/10.13031/2013.32748>

666 Wischmeier, W.H., Smith, D.D., 1978. Predicting rainfall erosion losses: a guide to conservation planning. U.S.
667 Department of Agriculture, Washington DC. <http://eprints.icrisat.ac.in/id/eprint/8473>

668 Woznicki, S.A., Nejadhashemi, A.P., 2013. Spatial and Temporal Variabilities of Sediment Delivery Ratio.
669 *Water Resour. Manag.* 27, 2483–2499. <https://doi.org/10.1007/s11269-013-0298-z>

670 Wu, C.S., Yang, S.L., Lei, Y.-P., 2012. Quantifying the anthropogenic and climatic impacts on water discharge
671 and sediment load in the Pearl River (Zhujiang), China (1954–2009). *J. Hydrol.* 452–453, 190–204.
672 <https://doi.org/10.1016/j.jhydrol.2012.05.064>

673 Wu, L., Long, T.Y., Liu, X., Ma, X.Y., 2013. Modeling impacts of sediment delivery ratio and land management
674 on adsorbed non-point source nitrogen and phosphorus load in a mountainous basin of the Three Gorges
675 reservoir area, China. *Environ. Earth Sci.* 70, 1405–1422. <https://dx.doi.org/10.1007/s12665-013-2227-0>

676 Xin, Z., Yu, X., Li, Q., Lu, X.X., 2011. Spatiotemporal variation in rainfall erosivity on the Chinese Loess
677 Plateau during the period 1956-2008. *Reg. Environ. Chang.* 11, 149–159.
678 <https://doi.org/10.1007/s10113-010-0127-3>

679 Yang, D., Kanae, S., Oki, T., Koike, T., Musiak, K., 2003. Global potential soil erosion with reference to land
680 use and climate changes. *Hydrol. Process.* 17(14), 2913–2928. <https://dx.doi.org/10.1002/hyp.1441>

681 Yang, F., Lu, C., 2015. Spatiotemporal variation and trends in rainfall erosivity in China's dryland region during
682 1961-2012. *Catena.* 133, 362–372. <https://doi.org/10.1016/j.catena.2015.06.005>

683 Zhang, B.H., Wu, X.G., X, G.F., 2015. Variation of water and sediment in rivers to sea in recent five Decades in
684 Zhejiang Province, *J. Sediemnt Res.* 6, 21-26 (in Chinese).
685 <https://doi.org/10.16239/j.cnki.0468-155x.2015.06.004>

686 Zhang, K.L., Shu, A.P., Xu, X.L., Yang, Q.K., Yu, B., 2008. Soil erodibility and its estimation for agricultural
687 soils in China. *J. Arid Environ.* 72, 1002–1011. <https://doi.org/10.1016/j.jaridenv.2007.11.018>

688 Zhang, W.B., Xie, Y., Liu, B.Y., 2002. Research evolution of rainfall erosivity. *J. Soil Water Conserv.* 16(5),
689 43–46 (in Chinese). <https://doi.org/10.3321/j.issn:1009-2242.2002.05.058>

690 Zhong, M., Ge, Y., Wang, W.W., 2013. Feature Extraction and Precision Analysis of the Eight Drainages in
691 Zhejiang Based on the SRTM DEM. *Sci. Tech. Engrg.* 13(22), 1671-1815 (in Chinese).
692 <https://doi.org/10.3969/j.issn.1671-1815.2013.22.033>

693

694

695

696

697 **Supplementary data**

698

699 **Text S1 Parameters in the RUSLE model**

700 **Rainfall erosivity factor (R):**

701 R, as the primary factor in the RUSLE model, reflects the ability of rainwater to strip,
702 move, and wash away soil under rainfall conditions, and describes the potential of rainstorms
703 to cause soil erosion. The half-month rainfall erosivity model by Zhang et al. (2002) is
704 described as follows:

$$705 \quad R = \alpha \sum_{j=1}^k (P_j)^\beta \quad (1)$$

$$706 \quad \beta = 0.8363 + \frac{18.144}{\bar{P}_{d12}} + \frac{24.455}{\bar{P}_{y12}} \quad (2)$$

$$707 \quad \alpha = 21.586\beta^{-7.1891} \quad (3)$$

708 Where R is the half-month rainfall erosivity ($MJ\ mm\ ha^{-1}\ h^{-1}\ yr^{-1}$) and P_j is the effective
709 rainfall for day j in one half-month of k days. If the actual rainfall is greater than the threshold
710 value of $12\ mm$, P_j is equal to the actual rainfall, otherwise, P_j is equal to zero (Xie et al.,
711 2000). The terms α and β are the undetermined parameters; \bar{P}_{d12} is the average daily rainfall
712 that is greater than $12\ mm$ and \bar{P}_{y12} is the annual average rainfall for days with rainfall
713 greater than $12\ mm$.

714 **Soil erodibility factor (K):**

715 The soil erodibility factor (K) measures the susceptibility of soil particles to detachment
716 and transportation during rainfall and runoff. The revised erosion/productivity impact
717 calculator (EPIC) model (Williams et al., 1984; Zhang et al., 2008):

$$718 \quad K_{EPIC} = \left\{ 0.2 + 0.3 \exp[0.0256SAN(1 - SIL/100)] \right\} * \left(\frac{SIL}{CLA + SIL} \right)^{0.3} \quad (4)$$
$$* \left[1.0 - \frac{0.25C}{C + \exp(3.72 - 2.95C)} \right] * \left[1.0 - \frac{0.7SN_1}{SN_1 + \exp(-5.51 + 22.9SN_1)} \right]$$

$$719 \quad K = (-0.01383 + 0.51575K_{EPIC}) * 0.1317 \quad (5)$$

720 Where K_{EPIC} and K is the soil erodibility factor ($t\ ha\ h\ ha^{-1}\ MJ^{-1}\ mm^{-1}$) before and after
 721 revision, respectively; SAN , SIL , CLA and C are the mass percentages of sand, silt, clay, and
 722 organic carbon, respectively; and SN_I is equal to $I-SAN/100$. In equation (5), the value 0.1317
 723 is the conversion factor from US units to SI units. Because the particle size classification
 724 standard used in the Second Soil Census data in China is based on the international system of
 725 soil texture, it is necessary to use logarithmic linear interpolation to transform the soil particle
 726 size data from the international system to the US system (Lu and Shen, 1992; Cai et al.,
 727 2003).

728 **Topographic factor (LS):**

729 The LS calculation was based on DEM (McCool et al, 1997; Renard et al., 1997) :

$$730 \quad L = \left(\frac{\lambda}{22.13}\right)^m \quad (6)$$

$$731 \quad S = \begin{cases} 10.8 \sin \theta + 0.03 & \theta < 9\% \\ 16.8 \sin \theta - 0.50 & \theta \geq 9\% \end{cases} \quad (7)$$

732 Where L is the slope length factor; S is the slope steepness factor; m is the slope length index
 733 and is acquired from the table by McCool et al. (1997); θ is the slope gradient ($^\circ$); and λ
 734 is the slope length (m). The parameters are computed based on the digital elevation model.

735 **Vegetation cover factor (C)**

736 For forestland, shrubland and grassland (Cai et al., 2000):

$$737 \quad C = \begin{cases} 1 & v = 0 \\ 0.6508 - 0.3436 \lg v & 0 < v \leq 78.3\% \\ 0 & v > 78.3\% \end{cases} \quad (8)$$

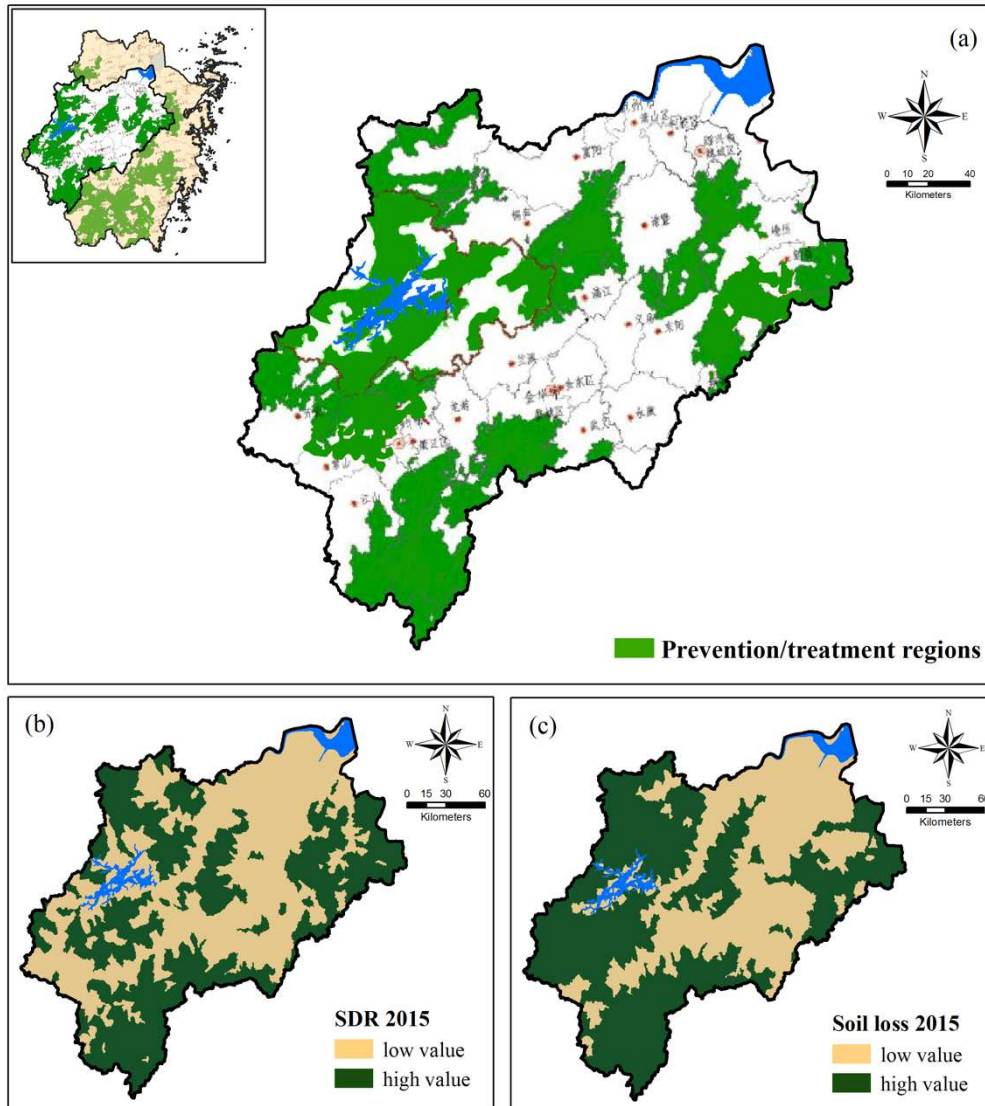
738 For dry land (Liu et al., 1999):

$$739 \quad C = 0.221 - 0.595 \log v \quad (9)$$

740 Where v is the vegetation cover factor of land use types. It is noteworthy that v is
 741 calculated as a proportion in equation (8) and as a percentage in equation (9).

742 **References:**

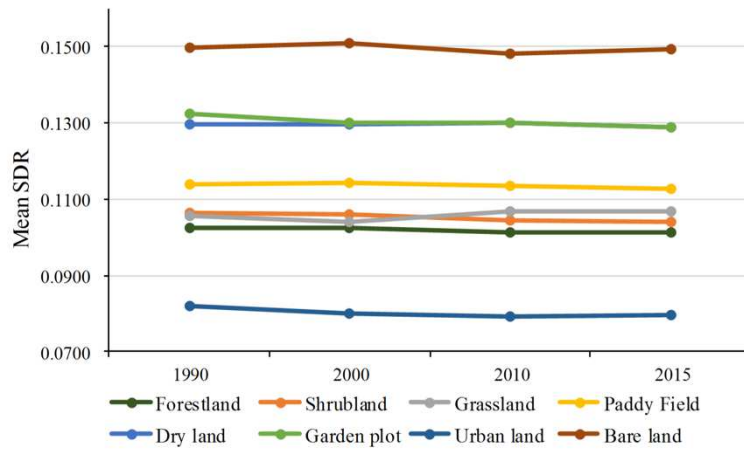
- 743 Cai, C.F., Ding, S.W., Shi, Z.H., Huang, L., Zhang, G.Y., 2000. Study of applying USLE and geographical
744 information system IDRISI to predict soil erosion in small watershed. *J. Soil Water Conserv.* 14,
745 19–24 (in Chinese).
- 746 Cai, Y.M., Zhang, K.L., Li, S.C., 2003. Study on the conversion of different soils texture. *Acta Pedol. Sin.*
747 40(4), 511–517 (in Chinese).
- 748 Liu, B.Z., Liu, S.H., Zheng, S.D., 1999. Soil conservation and coefficient of soil conservation of crops.
749 *Res. Soil Water Conserv.* 6 (2), 32–36 (in Chinese).
- 750 Lu, X.X., Shen, R., 1992. A preliminary study on the values K of soil erodibility factor. *J. Soil Water*
751 *Conserv.* 6(1), 63-70 (in Chinese).
- 752 McCool, D., et al., 1997. Slope-length and steepness factors (LS). *Predicting Soil Ero-sion by Water: A*
753 *Guide to Conservation Planning with the Revised Universal SoilLoss Equation (RUSLE)*. USDA
754 *Agriculture Handbook*.
- 755 Renard, K.G., et al., 1997. *Predicting Soil Erosion by Water: A Guide to Conservation Planning with the*
756 *Revised Universal Soil Loss Equation (RUSLE) (Agricultural Handbook 703)*. US Department of
757 *Agriculture, Washington, DC*.
- 758 Williams JR, Jones CA, Dyke PT. A modelling approach to determining the relationship between erosion
759 and soil productivity. *Trans ASAE* 1984;27(1):129–44.
- 760 Xie, Y., Liu, B.Y., Zhang, W.B., 2000. Study on standard of erosive rainfall. *J. Soil Water Conserv.* 14,
761 6–11 (in Chinese).
- 762 Zhang, K.L., Shu, A.P., Xu, X.L., Yang, Q.K., Yu, B., 2008. Soil erodibility and its estimation for
763 agricultural soils in China. *J. Arid Environ.* 72, 1002–1011.
- 764 Zhang, W.B., Xie, Y., Liu, B.Y., 2002. Research evolution of rainfall erosivity. *J. Soil Water Conserv.* 16
765 (5), 43–46. (in Chinese)



766

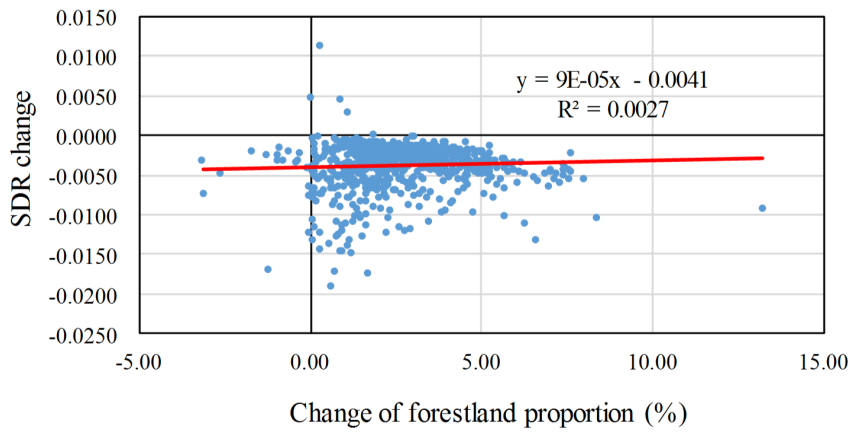
767 **Fig. S1.** (a) Published data: key prevention/treatment regions for soil erosion in Zhejiang
 768 Province and Qiantang River Basin; model results: spatial distribution of (b) SDR and (c) soil
 769 loss in 2015.

770 Note: Fig S1(a) was extracted from a published figure. (Zhejiang Water Resources
 771 Department, Zhejiang Development and Reform Commission, 2015, Announcement on key
 772 prevention/treatment regions and basic conditions of soil erosion in Zhejiang Province (in
 773 chinese).)



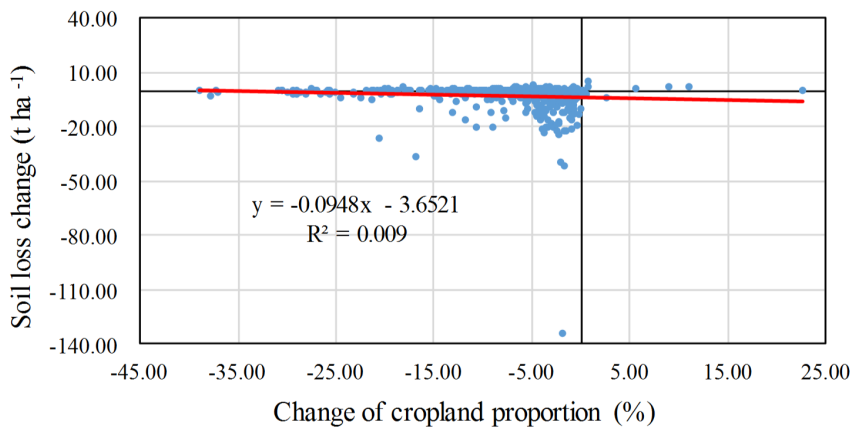
774

775 **Fig. S2.** The SDR of different land use types from 1990 to 2015 in the study basin.



776

777 **Fig. S3.** Relationship between change of forestland proportion and SDR change.



778

779 **Fig. S4.** Relationship between change of cropland proportion and soil loss change.

780

781 **Table S1**

782 The main data sources.

Data	Resolution	Source
Digital elevation model	90m	http://hydrosheds.org/
Precipitation	Daily (23 stations)	http://data.cma.cn/
Soil map	1:1,000,000	The Second Soil Survey in China
Land use map	30m	Zhejiang ecosystem assessment data
Vegetation coverage map	250m	Zhejiang ecosystem assessment data

783

784 **Table S2**

785 Observation data on sediment yield, SDR and soil loss in the Qiantang River Basin.

	Reference	Site (measured area)	Time	Observations
Sediment yield	MWR ¹	Lanxi (1.82)	1977-2015	1.24 t/ha
		Quzhou (0.54)	1958-2015	1.91t/ha
		Zhuji (0.17)	1956-2015	0.98t/ha
		Shangyu (0.45)	2012-2015	1.05t/ha
	Zhang et al.	Lanxi	1960-2012	242.38*10 ⁴ t
			1989-2000	206.00*10 ⁴ t
			2000-2009	118.46*10 ⁴ t
SDR	MWR ²	Qiantang (5.56)		0.11
	Li et al.	Lanxi		0.132
Soil loss	Li et al.	Qiantang		4688.73*10 ⁴ t
	MWR ²	Shuangyu	1958-2000	17.00 t/ha
		Lanxi	1977-2000	12.00 t/ha
Zhuji		1958-2000	10.10 t/ha	

786 **References:**

787 MWR¹:

788 Ministry of Water Resources of China (MWR), 2001-2015, China Gazette of River Sedimentation
789 2001-2015, China Water Power Press, Beijing, China (in Chinese).

790 Zhang, B.H., Wu, X.G., X, G.F., 2015, Variation of water and sediment in rivers to sea in recent five
791 Decades in Zhejiang Province, J. Sediemnt Res. 6, 21-26 (in chinese).

792 MWR²: Ministry of Water Resources of China (MWR), Chinese Academy of Sciences (CAS), Chinese
793 Academy of Engineering (CAE), 2010a. Control of soil erosion and ecological security in China: soil

794 erosion data volume. Control of Soil Erosion and Ecological Security in China. Science Press, Beijing
795 (in Chinese).

796 Li, Z.G., Liu B.Z., 2006. Calculation on soil erosion amount of main river basin in China. Sci Soil Water
797 Conserv. 4(2), 1-6 (in Chinese).

798

799 **Table S3**

800 The proportions of land use, the values of soil loss, SDR and sediment export and changes in
801 these values from 1990 to 2015 in the study area.

	1990	2000	2010	2015	1990-2000	2000-2010	2010-2015	1990-2015
Forestland (%)	59.63	59.88	61.91	62.38	0.25	2.03	0.47	2.75
Shrubland (%)	2.66	2.66	2.15	1.92	0.00	-0.51	-0.23	-0.74
Grassland (%)	2.83	2.49	1.27	1.06	-0.34	-1.22	-0.21	-1.77
Water (%)	5.52	5.50	5.39	5.26	-0.02	-0.11	-0.13	-0.26
Paddy field (%)	16.38	14.90	13.15	12.18	-1.48	-1.75	-0.97	-4.20
Dry land (%)	7.25	6.72	6.30	5.94	-0.53	-0.42	-0.36	-1.31
Garden plot (%)	1.45	1.81	1.21	1.14	0.36	-0.60	-0.07	-0.31
Urban land (%)	4.01	5.77	8.58	10.08	1.76	2.81	1.50	6.07
Bare land (%)	0.28	0.26	0.05	0.03	-0.02	-0.21	-0.02	-0.25
Change area (%)	-	-	-	-	3.01	8.01	2.33	12.50
SL (t ha-1 yr-1)	13.79	13.77	10.88	10.70	-0.02	-2.89	-0.18	-3.09
SDR	0.1040	0.1031	0.1011	0.1003	-0.0009	-0.0020	-0.0008	-0.0037
SE (t ha-1 yr-1)	1.69	1.69	1.26	1.22	0.00	-0.43	-0.04	-0.47

802 Note: SL: soil loss; SDR: sediment delivery ratio; SE: sediment export.

803

804

805

806

807

808

809

810

811

812 **Table S4**

813 Land use conversion matrix from 1990 to 2015 (in km²).

1990	2015									Total
	Forestland	Shrubland	Grassland	Water	Paddy Field	Dry land	Garden plot	Urban land	Bare land	
Forestland	25319.54	0.30	0.06	63.30	1.09	2.99	0.06	44.49	0.00	25431.83
Shrubland	276.07	801.82	0.06	5.87	0.29	0.41	0.31	48.80	0.04	1133.67
Grassland	185.29	2.29	440.47	3.50	112.67	241.64	5.44	215.78	0.07	1207.15
Water	4.15	0.27	0.49	2129.95	43.64	9.96	0.39	163.58	0.12	2352.55
Paddy Field	298.52	4.76	4.52	24.39	4754.63	383.55	126.13	1386.67	1.66	6984.83
Dry land	202.81	5.38	2.02	8.38	275.19	1857.44	35.22	706.82	0.18	3093.44
Garden plot	234.42	0.68	0.76	2.50	3.44	33.75	314.61	26.47	0.01	616.64
Urban land	4.83	0.12	0.24	5.69	5.39	3.00	1.13	1691.15	0.05	1711.60
Bare land	82.77	3.57	2.58	1.28	0.14	0.87	0.98	15.73	12.46	120.38
Total	26608.41	819.19	451.20	2244.86	5196.48	2533.61	484.27	4299.49	14.59	42652.09

814

815

816

817 **Table S5**

818 Sediment export change from different land use conversion from 1990 to 2015 (in t).

1990	2015								
	Forestland	Shrubland	Grassland	Water	Paddy field	Dry land	Garden plot	Urban land	Bare land
Forestland	-33459.83	9.02	5.51	-910.29	50.93	3852.64	62.32	283.99	10.40
Shrubland	-17841.11	-1897.07	5.15	-199.83	4.73	521.92	391.62	-1139.18	434.38
Grassland	-30366.20	-154.98	-1033.98	-154.21	-2637.08	111735.81	1869.26	-4003.67	323.51
Water	158.89	9.07	19.69	0.00	345.35	1934.15	347.37	916.92	0.35
Paddy field	-18958.19	-102.04	146.38	-423.03	-5218.11	172716.94	39958.70	-11085.24	4604.86
Dry land	-292483.68	-6230.22	-2136.09	-1327.81	-140993.24	-17787.59	-5874.53	-145570.75	313.19
Garden plot	-381033.47	-491.97	-480.64	-405.28	-3174.32	10574.82	-7443.58	-10526.74	15.88
Urban land	-44.10	1.68	7.84	-33.07	73.62	682.33	455.85	-577.72	52.99
Bare land	-1084218.79	-39844.60	-13057.97	-3526.92	-446.91	-1797.82	-8608.02	-40652.05	-1072.43

819

820